Trehalose facilitates DNA melting: a single-molecule optical tweezers study†

Sergey Bezrukavnikov,‡[a] Alireza Mashaghi,‡*[a] Roeland J. van Wijk,[a] Chan Gu,[b] Li Jiang Yang,[b] Yi Qin Gao[b] and Sander J. Tans[a]

Using optical tweezers, here we show that the overstretching transition force of double-stranded DNA (dsDNA) is lowered significantly by the addition of the disaccharide trehalose as well as certain polyol osmolytes. This effect is found to depend linearly on the logarithm of the trehalose concentration. We propose an entropic driving mechanism for the experimentally observed destabilization of dsDNA that is rooted in the higher affinity of the DNA bases for trehalose than for water, which promotes base exposure and DNA melting. Molecular dynamics simulation reveals the direct interaction of trehalose with nucleobases. Experiments with other osmolytes confirm that the extent of dsDNA destabilization is governed by the ratio between polar and apolar fractions of an osmolyte.

Introduction

The disaccharide trehalose (Fig. 1a) is a metabolite found in a wide range of organisms from different domains of life. It has been found that trehalose is synthesized specifically upon various stresses[1] and is thought to protect various cellular components such as DNA, proteins and membranes from loss of activity caused by heat, cold, dessication, dehydration, and oxidation.[2,3] *In vitro* experiments showed that trehalose can either stabilize or destabilize biomolecules depending on the substrate and the concentration of trehalose. Stabilization was observed with double-stranded DNA (dsDNA) in dry state, that is, at very high concentration of trehalose[3] and with folded proteins.[4,5] Unfolded proteins were reported to be stabilized by trehalose.[6,7] On the other hand, trehalose can destabilize folded proteins[8] and dsDNA in solution.[9] The extent of DNA destabilization due to trehalose depends on DNA length and on percent guanine–cytosine (GC) content as concluded from systematic thermal experiments on short duplexes.[10]

While the evidence for the influence of trehalose on proteins and nucleic acids is compelling, our understanding of the underlying mechanism is incomplete. Various mechanisms have been considered to explain the effect of trehalose on biomolecules,[1] including physically shielding parts of biomolecules and removing the hydration waters by replacing (direct interaction with biomolecule) or sequestering them (no direct interaction with biomolecule). Trehalose has been suggested to form hydrogen bonds (H-bonds) with the backbone phosphates and to dehydrate dsDNA molecules.[3] In these scenarios the repulsive electrostatic interactions between the phosphate groups may cause DNA melting.[3,11] One could also imagine a scenario in which trehalose competes with the complementary nucleobase in forming H-bonds and thereby hindering base-pairing and shielding single-stranded DNA (ssDNA).

Understanding the effect of trehalose and other osmolytes on the physicochemical properties of biomolecules is relevant not only for the biological context but also for technological applications.[12] Trehalose is commonly used in pharmaceutical industries and is contained in many therapeutic, cosmetic and food products.[13] It is also used in chemical industries for example to increase the yield in mass spectrometry[14] and DNA amplification. Trehalose increases the yield of polymerase chain reaction (PCR) by lowering the melting temperature of DNA.[15]

Here we address this problem by mechanically inducing melting of single dsDNA molecules with optical tweezers. Mechanical properties of biomolecules can be studied in real time using single molecule techniques such as optical tweezers. This method provides sub-piconewton resolution for force and sub-nanometer resolution in length scale. Optical tweezers have been extensively used to study the melting transition of single DNA molecules as well as the interaction of DNA with proteins and drugs[16–20] and are thus well suited to investigate the effect of trehalose on the melting of DNA. We use optical tweezers to grab the single DNA molecule at its ends and to induce its melting mechanically by stretching with different concentrations of
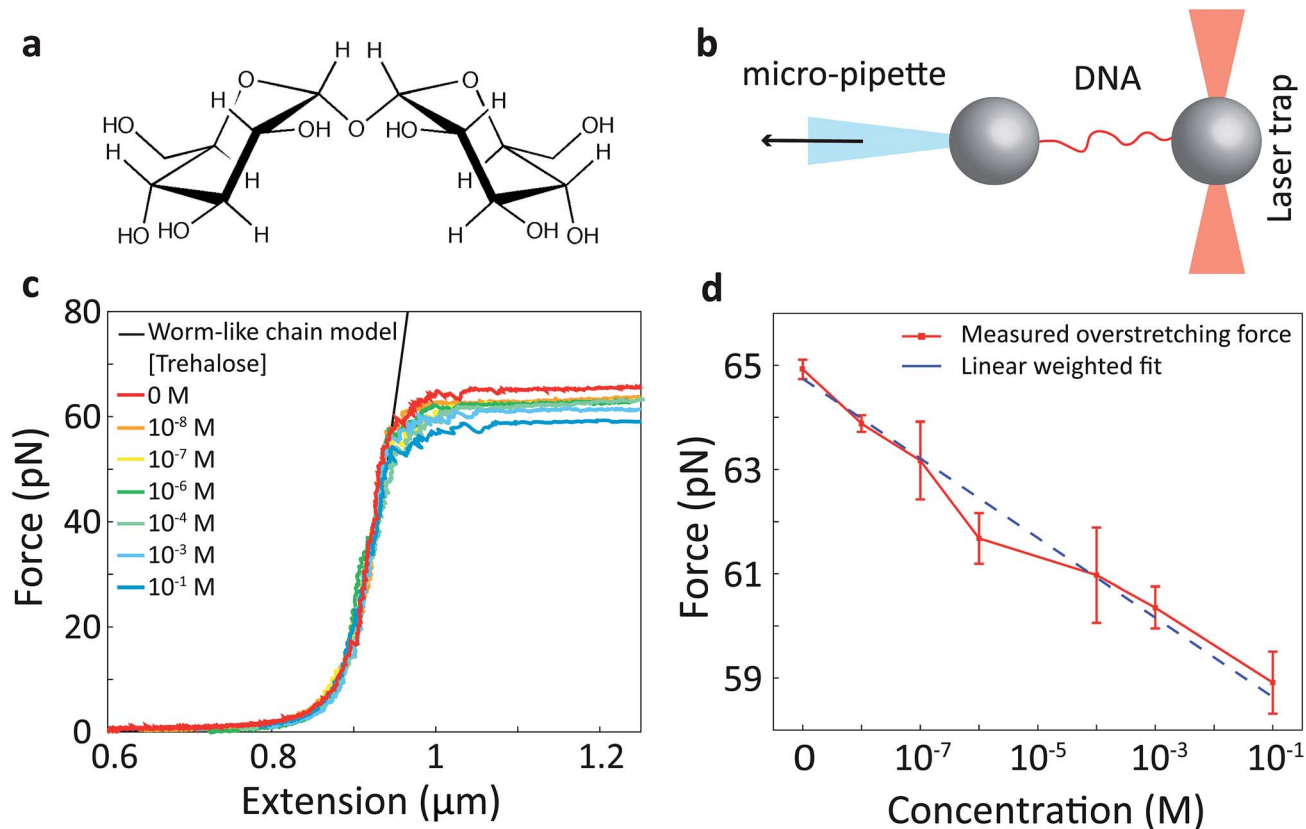
Fig. 1 (a) Chemical structure of trehalose. (b) A schematic drawing of the optical tweezers assay. (c) A force applied to DNA tether is plotted *versus* its extension. In the absence of trehalose the overstretching transition occurs at about 65 pN. The overstretching force decreases upon addition of trehalose. The black line is a worm-like chain model for the double-stranded DNA. (d) Overstretching force as a function of the log of trehalose concentration. The dashed line is a linear weighted fit ($R^2 = 0.9718$). The error bars indicate the standard deviations of the forces from various measurements.

trehalose added to the reaction buffer. We show that trehalose lowers the overstretching "transition"§ force of dsDNA. To explain the experimentally observed destabilization by trehalose, we looked at the thermodynamics of the system by adapting the model of DNA melting from Williams *et al.*[21] We also performed optical tweezers experiments on the effect of other molecules, such as: 1-propanol, 1-hexanol and glycerol, on DNA mechanics depending on the solubility of the additive. To obtain structural insights into the trehalose–DNA interaction we performed molecular dynamics (MD) simulations of ssDNA and dsDNA in the trehalose solution.

Methods

Functionalization of polystyrene beads

Carboxylated polystyrene beads (diameter ∼1.8 μm, Spherotech) were covalently attached to anti-digoxigenin (Anti-Dig) antibody (Roche Diagnostics) *via* carbodiimide reaction (Poly-Link Protein Coupling Kit, Polysciences Inc.). Briefly, the beads were washed and then mixed with freshly prepared 1-ethyl-3-(3-dimethylaminopropyl) carbodiimide and the antibody, and

mixture was incubated for 3 hours. Streptavidin-coated beads (diameter ∼1.8 μm, Spherotech) were stored at 4 °C until use. 2553 base pairs DNA handles were prepared and functionalized with digoxigenin (Dig) and biotin at 5′-ends of both strands as described in ref. 22. DNA-coated microspheres were made by mixing ∼70 ng of biotin–dsDNA–Dig and 1 μl Dig-coated beads in 10 μl HMK (50 mM HEPES, pH 7.6, 5 mM MgCl$_2$, 100 mM KCl) buffer. After a 30 minute incubation on a rotary mixer (4 °C), the beads were dissolved in 400 μl HMK buffer for use in optical tweezers experiments. Trehalose solution was made by dissolving trehalose dihydrate (Sigma Aldrich) in HMK buffer.

Force spectroscopy

Pulling experiments were performed at room temperature using a custom made optical tweezers apparatus (for details see ref. 22 and 23). Forces acting on the trapped bead lead to deflections of the laser beam, which were recorded with a quadrant photodiode at 50 Hz. Trap stiffness and sensitivity were measured to be 169 ± 24 pN μm^{-1} and 2.74 ± 0.24 V μm^{-1} respectively. The presence of trehalose barely affected the trap stiffness within the range of concentrations used (up to 0.1 M). A piezo stage (Physik Instrumente) was used to move the flow chamber and micropipette at a speed of 50 nm s^{-1}.

§ This is not a true thermodynamic transition, but we used this term since it is widely used in the field. The exact term should be "crossover".

A tether (dsDNA construct) is immobilized between two beads. Digoxigenin–dsDNA–biotin is immobilized between an anti-digoxigenin coated bead and a streptavidin coated bead *via* 5′-ends of its two strands. These connections enable easy and specific linking of both termini to the two types of beads used. The total numbers of DNA molecules studied at various solution conditions are listed in Table S1.†

Thermodynamic analysis

We adapted the model from Williams *et al.*[21] to understand the physical origin of dsDNA destabilization induced by trehalose. According to this model, the overstretching transition of dsDNA can be seen as force-induced melting which implies that the transition force should be dependent on the temperature. In the force (F)–temperature (T) space, at the boundary between the dsDNA regime and the ssDNA regime¶ the difference in total free energy between the two states is zero:[21]

$$\Delta G_{\text{tot}}(F,T) = 0 \tag{1}$$

Thus, the melting transition does not change the free energy of the system and the two states co-exist at the boundary. We assume that the total transition free energy can be written as the sum of the temperature-dependent transition free energy in the absence of force $\Delta G(T)$ and a force-dependent term $\Delta\Phi(F)$:

$$\Delta G_{\text{tot}}(F,T) = \Delta G(T) + \Delta\Phi(F) \tag{2}$$

$$\Delta G_{\text{tot}}(F,T) = \Delta S(T_{\text{m}}^0)(T_{\text{m}}^0 - T) - \frac{\Delta C_{\text{p}}}{2}\frac{(T - T_{\text{m}}^0)^2}{T_{\text{m}}^0} + \Delta\Phi(F) \tag{3}$$

where $\Delta S(T)$ denotes the total transition entropy of the system, ΔC_{p} is the change in the heat capacity of the system during the transition, $\Delta\Phi(F)$ is a one-dimensional thermodynamic potential analogous to the Gibbs free energy and T_{m}^0 is the temperature at which the melting transition occurs in the absence of force. At room temperature, stretching of the dsDNA from its two ends using optical tweezers will result in melting at a certain force which depends on the concentration of trehalose. At the melting transition we have:

$$\Delta S(T_{\text{m}}^0)(T - T_{\text{m}}^0) + \frac{\Delta C_{\text{p}}}{2}\frac{(T - T_{\text{m}}^0)^2}{T_{\text{m}}^0} = \Delta\Phi(F) \tag{4}$$

The right side of the identity can be derived directly from integration of the force–extension curve fits.

Force–extension optical tweezers data for dsDNA behaviour was fitted to the generalized discrete worm-like chain model (WLC) proposed by Manghi *et al.*[24] According to this model, the following relation between extension and force acting on the molecule is valid for pure dsDNA (eqn (47) in Manghi *et al.*[24]):

¶ Strictly speaking, state of DNA after transition depends on a variety of factors. For more details see Discussion. It does not affect the validity of method we used, thus we will refer to overstretched DNA as ssDNA for simplicity.

$$\frac{z}{a_{\text{Ds}}N} = \left(1 + \frac{F}{\tilde{E}_{\text{Ds}}} - \frac{1}{2\alpha_{\text{Ds}}}\right)\varphi_{\text{Ds}} + \gamma\left(1 - \frac{1}{2\alpha_{\text{Ss}}}\right)\varphi_{\text{Ss}} + \frac{\langle\sigma_i\sigma_{i+1}\rangle - 1}{4}$$
$$\times\left(\frac{1}{2\alpha_{\text{Ds}}}\frac{\kappa_{\text{Ds}} - \kappa_{\text{DsSs}}}{\kappa_{\text{DsSs}} + F/2 + \alpha_{\text{Ds}}} + \frac{\gamma}{2\alpha_{\text{Ss}}}\frac{\kappa_{\text{Ss}} - \kappa_{\text{DsSs}}}{\kappa_{\text{DsSs}} + \gamma F/2 + \alpha_{\text{Ss}}}\right) \tag{5}$$

where indices 'Ds' and 'Ss' are used, respectively, for dsDNA and ssDNA states. F denotes force, z – extension, N – number of residues in DNA, a – monomer size, $\tilde{E}$ – a dimensional stretching modulus, $\gamma = \frac{a_{\text{Ss}}}{a_{\text{Ds}}}$, $\alpha_{\text{Ds}} = \sqrt{\kappa_{\text{Ds}}F + \left(\frac{F}{2}\right)^2}$, $\alpha_{\text{Ss}} = \sqrt{\kappa_{\text{Ss}}\gamma F + \left(\frac{\gamma F}{2}\right)^2}$, κ – a dimensional bending modulus for dsDNA and ssDNA states. $\varphi(F)$ denotes the fraction of base pairs in certain state of DNA. σ_i is an Ising variable that denotes the state (broken or unbroken) of each base pair in DNA. $\langle\sigma_i\sigma_{i+1}\rangle$ is the two-point correlation function. Here we used $a_{\text{Ds}} = 0.34$ nm, $a_{\text{Ss}} = 0.62$ nm, $\tilde{E}_{\text{Ds}} = 101$, $\gamma = 1.829$, $\kappa_{\text{Ds}} = 147$, $\kappa_{\text{Ss}} = 1.28$.

The part of the data after overstretching transition force was fitted to the discrete Marko–Siggia WLC interpolation with non-linear elasticity.[24] It describes the elastic response of ssDNA with this relation (eqn (16) in Manghi *et al.*[24]):

$$\frac{aF}{k_{\text{B}}T} = \frac{z}{L}\left(1 + U_{\text{nl}}(F)\right)\left(3\frac{1 - u(\kappa)}{1 + u(\kappa)} - \frac{1}{\sqrt{1 + 4\kappa^2}}\right)$$
$$+ \sqrt{\frac{1}{[1 - z(1 + U_{\text{nl}}(F))/L]^2} + 4\kappa^2} - \sqrt{1 + 4\kappa^2} \tag{6}$$

where F denotes force, z – extension, L – contour length, κ – a dimensional bending modulus, and a – monomer size. $u(\kappa)$ is the Langevin function defined as $u(\kappa) = \coth\kappa - 1/\kappa$, and $U_{\text{nl}}(F)$ is a non-linear stretching polynomial. Here we used $L = 920$ nm, $\kappa = 1.28$, $a = 0.665$ nm.

By directly integrating the WLC curves, one can find the force-dependent free energy change $\Delta\Phi(F)$ associated with the melting transition of the DNA:

$$\Delta\Phi(F) = \int_0^F\left[z_{\text{Ss}}(F') - z_{\text{Ds}}(F')\right]\mathrm{d}F' \tag{7}$$

Integrations for the Gibbs free energy were performed over a 0–100 pN interval to find $\Delta\Phi(F)$. Using a melting temperature of $T_{\text{m}} = 100\ ^\circ\text{C}$ from base-stacking calculations,[19] room temperature of $T = 21\ ^\circ\text{C}$ and $\Delta S(T_{\text{m}}) = 24.7$ cal mol^{-1} K^{-1} bp, one can thus numerically solve the overstretching force associated with each value of ΔC_{p} for different trehalose concentrations using eqn (3).

MD simulations

Five different molecules, which are 30-mer AT (both ds and ssDNA), 30-mer GC (both ds and ssDNA) and 33-mer dsDNA with GC-content of 50% were studied in the molecular dynamics simulation. They were all solvated in either pure water or 0.5 M trehalose aqueous solutions, namely, resulting in an overall of ten simulation systems. All MD simulations were conducted using AMBER11 suite of programs.[25] The SPCE

Table 1 Parameters for individual MD simulations

DNA Sequence	Solvent	Trehalose	Water	Salt	Duration (ns)
dsAT 5′-ATATATATATATAT	Pure water	—	11 673	58	95
ATATATATATATATAT-3′	0.5 M trehalose	108	11 565	58	45
dsGC 5′-GCGCGCGCGCGCGCGCGCGC	Pure water	—	8417	58	108
GCGCGCGCGC-3′	0.5 M trehalose	78	8339	58	70
ds50%GC 5′-GAGATGCTAACC	Pure water	—	9929	64	156
CTGATCGCTGATTCCTTGGAC-3′	0.5 M trehalose	92	9837	64	70
ssAT 5′-ATATATATATATATAT	Pure water	—	8941	29	168
ATATATATATAT-3′	0.5 M trehalose	83	8912	29	66
ssGC 5′-GCGCGCGCGCGCGCGCGCGCG	Pure water	—	8947	29	145
CGCGCGCGC-3′	0.5 M trehalose	83	8918	29	65

model[26] was used to describe the explicit water solvent. Nucleic acid and trehalose force field parameters were taken from the AMBER ff10 parameter set[27] and GLYCAM06,[28] respectively. In each system, the canonical B form of DNA was used as the initial structure and then immersed into a cubic box containing water and trehalose. The detailed parameters of the simulation systems are listed in Table 1.

For each system, the simulation procedure included the energy minimization, heating up and the equilibration using the NPT ensemble. First, the system was minimized through 500 steps of steepest descent minimization and the following 500 steps of conjugate gradient minimization with DNA being fixed using harmonic restraints. Then the restraints on DNA were released and the system was minimized using 1000 steps of the steepest descent and then 1500 steps of conjugate gradient minimization. In order to relax the system further (especially the solvent molecules), it was heated to 360 K first and equilibrated at this temperature for 300 ps, then it was cooled down to 300 K. Finally, production runs were performed and the temperature of all systems was maintained at 300 K using the Langevin dynamics with a friction coefficient of 5 ps^{-1}. The pressure of the system was adjusted to 1 atm by Berendsen weak-coupling[29] algorithm with relaxation time constants of 2 ps.

In all simulations, the SHAKE algorithm[30] was used in order to restraint all covalent bonds involving hydrogen. Therefore, all dynamics employed an integral time step of 2 fs. Periodic boundary conditions were used and the particle-mesh Ewald(PME)[31] with a direct space cutoff of 10 Å was utilized to treat long-range electrostatic interactions.

The figures of DNA–trehalose interaction were made in PyMOL.[32]

Results

Single molecule mechanics of dsDNA

We used optical tweezers to measure the mechanical response of dsDNA (2553 base pairs, GC content ∼51%) to applied forces. In these experiments, the DNA was grabbed at its ends by immobilizing the end of one strand on each side to micron-sized spheres, thus leaving the DNA torsionally unconstrained and end-opened (Fig. 1b). A typical force–extension stretching curve is presented in Fig. 1c (red curve). In the stretching curve, when the force on the DNA increases, overstretching occurred at about 65 pN as reported previously.[33,34] During the overstretching transition the length of the DNA increased, while force barely changed, indicating alteration of structure. We note that the force during the overstretching was approximated to be constant. The overstretching force for each stretching curve was defined as an average force value for the transition region between the fitting curves of dsDNA and ssDNA.

The relaxation curves, when the beads were brought close together again, exhibited significant hysteresis[19] (Fig. S1†). A consecutive stretching after 5 s waiting time at zero force resulted again in a similar curve followed by overstretching which indicates that the single-stranded fragments of DNA annealed to regenerate the double stranded conformation.

DNA stretching in the presence of trehalose

The trehalose experiments were performed in three steps. First the DNA was stretched and relaxed multiple times in the absence of trehalose in HMK buffer. Next, HMK buffer containing trehalose was flown into the sample chamber. Finally, the DNA was stretched and relaxed multiple times to assess the effect of trehalose. Without the disaccharide, the DNA compliance at low forces is in line with a worm-like chain model,[35] and at force about 65 pN the extended DNA molecule undergoes the overstretching transition. When trehalose is added to the system, DNA behavior does not change at low forces. However, the magnitude of the overstretching force was significantly affected by the presence of trehalose (Fig. 1c), and decreased by nearly 5 pN over the range of trehalose concentrations studied (up to 100 mM). Results from experiments (Fig. 1d) show that the overstretching force decreases almost linearly with the log of the concentration of trehalose. However, relaxation curves of DNA did not exhibit more hysteresis in the presence of trehalose (data not shown).

Effect of other amphiphiles on dsDNA mechanics

While it has been shown that different osmolytes have different effects on the stability of the substrate,[7] a detailed mechanism has not yet been determined. For instance, it is unclear how specific structural features of the osmolyte give rise to the
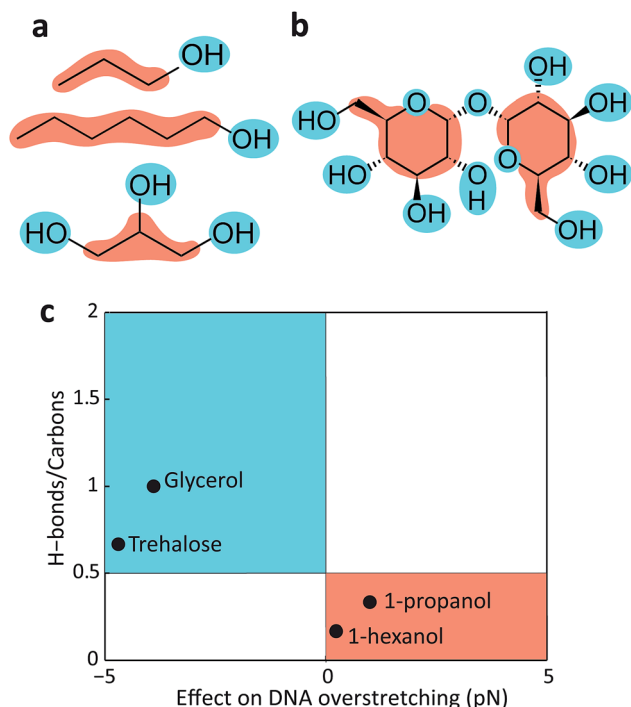
Fig. 2 Effect on dsDNA overstretching force for various amphiphiles. (a) From top to bottom: 1-propanol, 1-hexanol, glycerol. (b) Trehalose. Hydrophilic parts of the molecules are highlighted in blue and hydrophobic parts in orange. (c) Diagram showing the relationship between the effect of each molecule on dsDNA overstretching force (x axis) versus the ratio of the amount of possible hydrogen bonds to the number of carbons present in the molecule (H-bonds/carbons, y axis).

observed effects. In order to investigate the importance of the chemical structure of osmolytes on the effect they have on dsDNA mechanics, we have performed pulling experiments under similar conditions, adding solutes that exhibit different ratios of hydrophobic and hydrophilic groups (Fig. 2a and b).

For the same concentration of osmolyte (1 mM), we observed almost no effect on the overstretching force with 1-propanol and 1-hexanol, while a decrease in order of 4 pN was detected with glycerol (Fig. 2c).

MD simulations

The optical tweezers experiments show the destabilizing effect of trehalose on dsDNA molecule but the details of this interaction remain unclear. To find out if trehalose interacts directly with the DNA, we performed molecular dynamics simulations on ssDNA and dsDNA with 30-mer AT, 30-mer GC and 33-mer with 50%GC in the presence of 0.5 M trehalose (Fig. 3). We determined the number of hydrogen bonds between trehalose and DNA during the simulation for the different DNA molecules, and found that trehalose interacted in majority with the backbone in the case of dsDNA whereas for ssDNA trehalose interacted in majority with its bases (Fig. S2†), leading to significant elongation of the ssDNA (Fig. 3b). As compared to ssDNA in the absence of trehalose we observed ~30% and ~50% increase in the average end-to-end distances for AT and

GC ssDNA molecules in the presence of 0.5 M trehalose. In contrast, for dsDNA a reduction in the end-to-end distances was observed. Notably, during the simulation trehalose formed more hydrogen bonds with GC DNA, than with AT DNA (Fig. S3†), that is consistent with more pronounced effect of trehalose on GC DNA.[10]

We also analyzed the effect of trehalose on the surrounding aqueous environment by calculating the radial distribution function (RDF) for water molecules and DNA in the presence and in the absence of trehalose in the simulation box (Fig. S4†). Addition of trehalose lowers RDF without affecting its shape. It suggests that trehalose replaces some of the waters in the vicinity of DNA. It is in line with direct interaction between trehalose and nucleobases *via* hydrogen bonds.

Discussion

Physical mechanism of trehalose induced dsDNA destabilization

At the overstretching force, dsDNA undergo structural changes that depend on the experimental conditions. For the torsionally unconstrained DNA, two types of transitions can occur: unpeeling of strands from the ends of the molecule, that involves disruption of base pairs and yields ssDNA; and the so-called "B-to-S" transition‖, where the DNA helix unwinds with the base pairs remaining intact,[36,37] yielding another dsDNA structure called S-DNA.

As an indicator of the occurrence of certain DNA structures at the overstretching we considered the presence or absence of hysteresis in the relaxation curve. The B-to-S transition is non-hysteretic, while the unpeeling transition exhibits significant hysteresis in the relaxation curve.[38] The presence of hysteresis in our data (Fig. S1†) suggests that base pairing is indeed disrupted during the overstretching. With our DNA sequence and within our experimental conditions, we never observed a stretching curve without the hysteresis in relaxation phase. This indicates the transition is not exclusively B-to-S. More likely, we observe a mixture of unpeeled DNA and S-DNA that coexist in one DNA molecule. This hypothesis is also supported by our fits of DNA stretching curves after overstretching transition (see eqn (6)), which yield bending modulus $\kappa = 1.28$ that is equal to and monomer size $a = 0.665$ nm that is slightly less than the values reported by Manghi et al.[24] ($\kappa = 1.28$, $a = 0.7$ nm) for ssDNA. The competition between different overstretching mechanisms has been demonstrated recently experimentally with an arbitrary DNA sequence in conditions similar to ours by King et al.[36]

The DNA overstretching occurs at applied force that varies negligibly during the transition and at constant temperature, and it has already been characterized as force-induced melting process.[21] From a thermodynamics point of view, during the melting the Gibbs free energy does not change while the enthalpy and the entropy of the material do increase. Melting occurs when the Gibbs free energy of the ssDNA becomes lower than that of the dsDNA. The temperature at which this occurs

‖ B-DNA is the name for the most common dsDNA structure under the conditions found in cells.
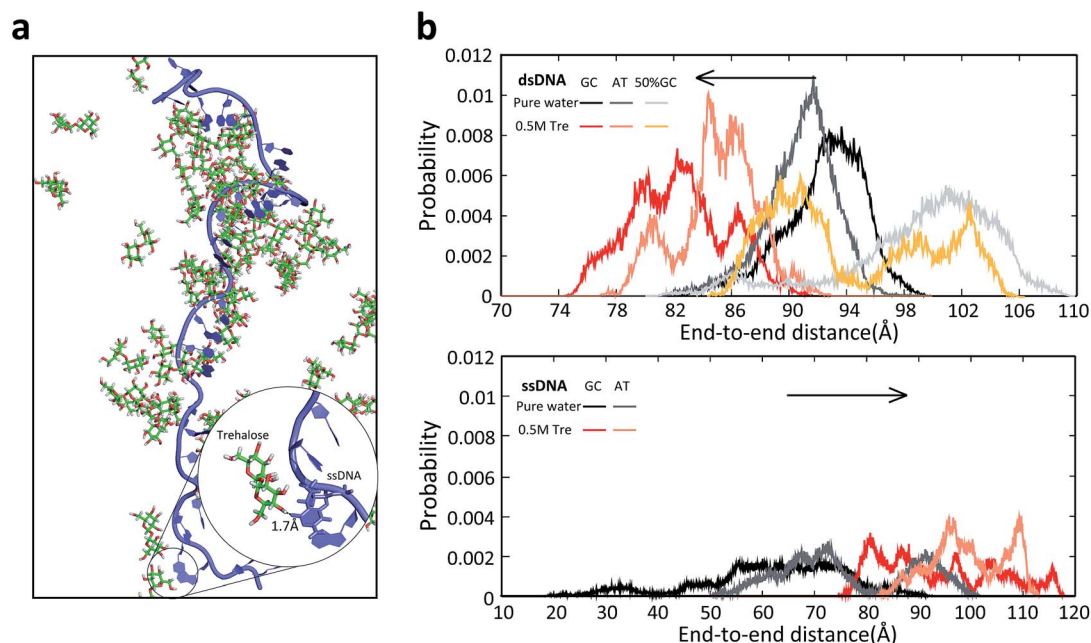
Fig. 3 Results from molecular dynamics simulation of trehalose–DNA system. (a) Direct interaction of trehalose with nucleobases in ssDNA. (b) The effect of trehalose (Tre) on end-to-end distance of ss and dsDNA. This distance is defined as the distance between midpoints of $C_{\bar{3}}$ in the furan rings of the first and the last base pair. The distribution of end-to-end distances is plotted for dsDNA (top) and for ssDNA (bottom) without trehalose (black trace for GC, dark grey for AT and light grey for 50%GC DNA) and in the presence of 0.5 M trehalose (red trace for GC, orange for AT and yellow for 50%GC DNA). While trehalose reduces the average end-to-end distance of dsDNA, it enhances the end-to-end distance of ssDNA. In both cases the effect on GC DNA is more pronounced than AT DNA.

depends on the external force and the buffer composition. At zero force the melting temperature (T_{m}^{0}) is well above the ambient temperature and dsDNA is stable. At a force of 65 pN (overstretching force), the melting temperature $T_{\mathrm{m}}^{F_{\mathrm{os}}}$ equals the ambient temperature and the transition occurs. Trehalose has been reported as a potent PCR enhancer, which indicates that it lowers T_{m}^{0}.[9] Under similar buffer conditions as ours in bulk assays, the zero-force melting temperature of dsDNA molecules with similar GC content was found to decrease by 4.4 °C per molar concentration of trehalose.[10] The extent of this change was found to depend strongly on the GC content but only minimally on the DNA length.[10] Over the range of trehalose concentrations assayed here (from 0 to 100 mM), these results would imply a decrease of the order of 1 °C in the melting temperature (T_{m}^{0}) and in $T_{\mathrm{m}}^{F_{\mathrm{os}}}$ in our experiments.

A previous experimental analysis of the dependence of the overstretching force on temperature in optical tweezers assays[21] can also be compared with our data. Given the decreases in overstretching force observed here, this previous work suggests a much larger decrease of the melting temperature of about 15 °C. This indicates that the 1 °C change in the melting temperature afforded by enthalpic and entropic changes associated with breaking the base pairing alone cannot account for the significant change in overstretching forces measured in Fig. 1d. Another aspect of the stability of molecules is their interaction with the solvent. DNA melting results in the exposure of the nucleobases which due to the interactions with their hydrophobic surfaces have an effect on the interfacial water.[39,40] This transition affects the degrees of freedom of the water, and

hence the heat capacity of the entire system, which is the energy needed to increase the temperature (kinetic energy per degree of freedom) of the system by one degree. We note that the hydrophobicity of nucleobases is a complicated concept. Bases can be considered hydrophilic because they can form hydrogen bonds and are water soluble. However, they also possess considerable hydrophobic surfaces that provide significant contribution to DNA duplex formation.[41]

The contribution of the surrounding aqueous environment to heat capacity effects for DNA melting has already been underscored in the literature: Rouzina et al.[42] argue that the entropic change associated with changes in heat capacity upon melting ΔC_{p} of DNA can be a factor 2–4 times larger than the entropic change associated with only breaking the base pairing $\Delta S_{\mathrm{bp}} \approx 25$ cal mol^{-1} K^{-1}. Therefore the surrounding environment significantly contributes to the total entropy of the system (ΔS), an effect that changes with varying solution conditions. They also reason that an increase in hydrophobicity can greatly increase this heat capacity. We note that this effect could not be observed in PCR experiments or other experiments in which the system is observed in thermostatic conditions and not during heating and cooling.

Trehalose provides a hydrophobic environment for DNA

DNA basepairing in aqueous buffer is enthalpically driven by establishing the hydrogen bonds between the bases. Entropy also has a known effect on the stability of double-stranded DNA. For example the chain conformational entropy reduces upon

transition from ssDNA to dsDNA.[43] The reduction of entropy has been attributed to a reduced configuration space for hydrogen or alternatively to an increase of many-body correlations.[44] The arrangement of water molecules at the interface with DNA, *e.g.* in the grooves,[39,45] will also have an entropic contribution. The water arrangement entropy could be influenced by the change in the composition of aqueous buffer, for example by addition of amphiphilic molecules[40] and solutes.[46]

Trehalose possesses both hydrophobic and hydrophilic moieties, being a moderate amphiphile.[47] Hydrophobicity on the molecular scale is widely believed to have an entropic origin,[46,48,49] particularly at room temperature. To test if an increase in hydrophobicity due to trehalose could account for the changes in the overstretching force, we adapted the model from Williams *et al.*[21] It assumes that DNA melting occurs during the overstretching transition and that the total transition free energy can be written as the sum of a temperature-dependent term in the absence of force and a force-dependent term. Using this model, we can estimate what changes in heat capacity – and the consequent change in the system's entropy – would explain the measured DNA overstretching forces. Although the DNA used and the buffer conditions in Williams *et al.*[21] are different from ours, a comparative assessment can still be made about the effects of increasing trehalose concentration on the overstretching force.

We used the discrete worm-like chain (WLC) to fit data of the dsDNA and ssDNA (Fig. 4a). By directly integrating the WLC curves, one can find the force-dependent free energy change $\Delta\Phi(F)$ associated with the melting transition of the DNA as shown in eqn (7). Thus one can numerically solve the over-stretching force associated with each value of ΔC_p for different trehalose concentrations using eqn (4).

To illustrate, $\Delta G_{tot}(F,T)$ is plotted in Fig. 4b at room temperature $T = 21\,^{\circ}$C, $\Delta C_p = 60$ cal mol^{-1} K^{-1} bp and $\Delta S(T_m^0) = 24.7$ cal mol^{-1} K^{-1} bp. The orange dashed line marks the transition of the DNA molecule favouring the double-stranded state at lower forces and the single-stranded state at higher forces. Changes in T_m over a reasonable range (of order $1\,^{\circ}$C, see ref. 21) show little effect on the temperature-dependent part of the transition free energy $\Delta G(T)$ (Fig. 4d) and hence the force required for the melting transition (Fig. 4c). The left side of the eqn (4) is a linear function of ΔC_p. The dependence of the overstretching force and consequently $\Delta\Phi(F)$, on the trehalose concentration, implies that ΔC_p has to be dependent on the concentration of trehalose as well. Changes in C_p over a reasonable range (see ref. 42) do result in significant adjustments of $\Delta G(T)$ (Fig. 4d). Moreover, the model provides a good quantitative fit to the measured overstretching force (Fig. 1d), for a linear dependence of ΔC_p on the log[trehalose] (Fig. 4e).

A change in ΔC_p as a function of trehalose concentration indicates a change in the number of degrees of freedom of the system and consequently the system entropy, that depends on heat capacity change as follows:[21]

$$\Delta S = \Delta S(T_m) + \Delta C_p \times \ln \frac{T}{T_m} \qquad (8)$$
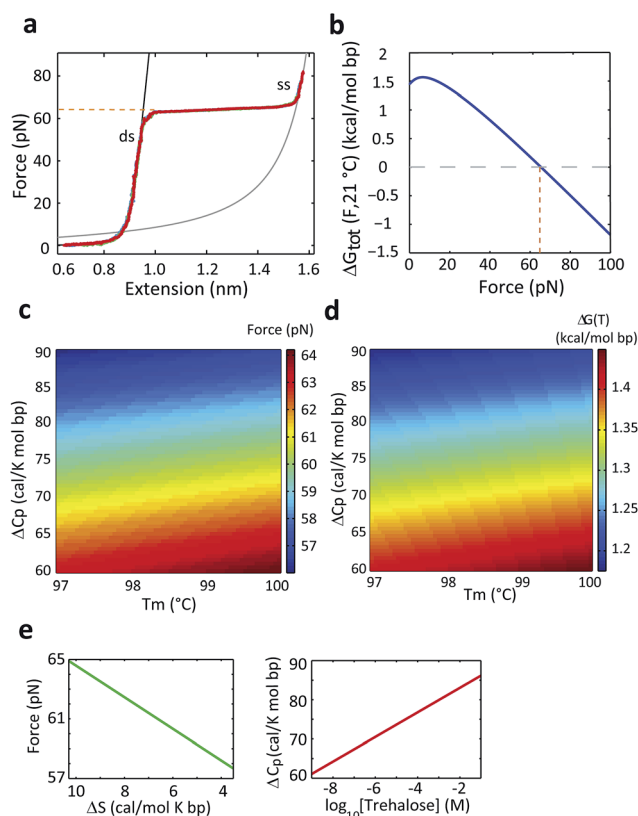

Fig. 4 Physical mechanism of trehalose induced destabilization of double-stranded DNA. (a) A typical force–extension plot is shown. Black line is the WLC model for dsDNA, grey line – for ssDNA. The dashed line indicates the force at which the DNA melting from dsDNA to ssDNA occurs at room temperature (21 $^{\circ}$C) in the absence of trehalose. (b) The total free energy difference ($\Delta G_{tot}(F,T)$), as a function of force at room temperature, $T_m = 100\,^{\circ}$C and at $\Delta C_p = 60$ cal mol^{-1} K^{-1} bp. This value of ΔC_p corresponds to the DNA in the absence of trehalose as calculated in ref. 21. (c) Color map of the force required for melting as a function of T_m and ΔC_p (eqn (4) and (5)). (d) Color map of the temperature-dependent transition free energy as a function of T_m and ΔC_p. (e) Left panel: overstretching force of DNA measured for different concentrations of trehalose is plotted *versus* calculated total transition entropy from dsDNA to ssDNA in solution (ΔS). Right panel: DNA heat capacity change upon melting (ΔC_p) *versus* the concentration of trehalose. For the thermodynamic model to numerically fit the measured overstretching forces (Fig. 1d), it would have to produce a linear increase in ΔC_p with the log of the trehalose concentration, as indicated here. ΔC_p goes down linearly by increasing ΔS *i.e.* ΔS is proportional to the log of [trehalose].

Here, an increasing ΔC_p corresponds to decreasing transition entropy (see eqn (8); note that for $T < T_m$, $\ln \frac{T}{T_m}$ is negative). These findings indicate that a dependence of C_p on trehalose concentration could explain the observed effect of trehalose on the overstretching force (Fig. 1d).

These thermodynamic considerations provide physical insight into the trehalose-mediated DNA melting process. However, multiple underlying molecular (chemical) mechanisms can be envisioned. Water–trehalose interactions (competition for water with DNA) leading to trehalose-mediated sequestering of water molecules could promote a dehydration

of DNA molecule, that is assumed to destabilize DNA duplex,[11] while providing a relatively hydrophobic environment for the DNA bases. Alternatively, due to amphiphilic properties of trehalose,[47] its direct interaction with the DNA bases (either *via* H-bonds or van der Waals interactions) leading to replacement of water by trehalose in the vicinity of the DNA could provide more hydrophobic interface for bases, and at the same time provide more hydrophilic interface for water. With the results discussed so far we cannot sketch an atomistic picture of the process, which we aimed to address by investigating some of the molecular motifs found in polyol osmolytes and by using MD simulations.

The ratio between polar and apolar fractions of an osmolyte determines the effect on the DNA

To explain the more prominent dsDNA destabilization caused by glycerol and trehalose and the lack of effect with 1-propanol and 1-hexanol we consider the solubility of the additives. Water is structured around the osmolyte and it results in the heat capacity change ΔC_p, which is positive for apolar solutes and negative for polar solutes.[50] The amount of polar and apolar groups in the additive can be seen as an indicator of a (de-) stabilization effect on DNA double helix. As a rough estimate of polar and apolar fraction we have considered the ratio of the amount of possible hydrogen bonds to the number of carbons present in each molecule (Fig. 2a and b).

We find that this ratio correlates well with the overstretching force (Fig. 2c). In contrast, the total number of polar or apolar groups do not correlate well with the overstretching force. For example, glycerol (which reduces DNA overstretching force) and 1-propanol (which has no effect on it) contain the same number of apolar groups. Moreover, trehalose and glycerol contain a very different number of polar groups but reduce the overstretching force to similar extent. These data suggest that neither the hydrophilicity nor the hydrophobicity of the molecule determines the effect, but the ratio between the parts is important. The data suggest that molecules with the particular ratio, such as trehalose (and glycerol), are more effective at providing a bridging interface between the hydrophobic surface area of the DNA bases and the surrounding water, lowering the transition energy from dsDNA to ssDNA and decreasing the overstretching force.

Trehalose binds the nucleobases

The results from MD simulations show that trehalose interacts directly with the bases of ssDNA in aqueous solution. It leads to elongation of ssDNA, that indicates the stiffening of the polymer upon trehalose addition. In the case of dsDNA, trehalose causes the increase in flexibility of the polymer, that is in agreement with experimentally observed dsDNA destabilization. From these data, a simple mechanism is proposed: thermal fluctuations (particularly when the transition barrier between ssDNA and dsDNA is suppressed in the presence of mechanical force) disrupt the base-pairing in the dsDNA leading to exposure of the bases (base flipping). Trehalose then interacts with the bases and increases the likelihood of

the flipped-out state. This can explain the experimental observations of the reductions in overstretching forces of dsDNA. The more prominent effect in the case of CG is in agreement with the larger hydrophobic surface areas of guanine and cytosine, particularly the stacking areas.[51,52]

Conclusion

Our single molecule optical tweezers study, together with the thermodynamic analysis and molecular dynamics simulations provide a general mechanism that explains the influence of trehalose on biomolecules. The data indicate that – due to the presence of hydrophobic moieties – trehalose interacts more with hydrophobic parts of biomolecules than water and favours the exposure of hydrophobic fragments. Furthermore its amphiphilic character allows trehalose to bridge between hydrophobic moieties and surrounding water resulting in an entropically favored interface.

Acknowledgements

References

1 N. Jain and I. Roy, *Protein Sci.*, 2009, **18**, 24–36.
2 A. Elbein, Y. Pan, I. Pastuszak and D. Carroll, *Glycobiology*, 2003, **13**, 17R–27R.
3 B. Zhu, T. Furuki, T. Okuda and M. Sakurai, *J. Phys. Chem. B*, 2007, **111**, 5542–5544.
4 J. Kaushik and R. Bhat, *J. Biol. Chem.*, 2003, **278**, 26458–26465.
5 E. Melo, L. Chen, J. Cabral, P. Fojan, S. Petersen and D. Otzen, *Biochemistry*, 2003, **42**, 7611–7617.
6 M. Tanaka, Y. Machida, S. Niu, T. Ikeda, N. Jana, H. Doi, M. Kurosawa, M. Nekooki and N. Nukina, *Nat. Med.*, 2004, **10**, 148–154.
7 M. Singer and S. Lindquist, *Mol. Cell*, 1998, **1**, 639–648.
8 S. Habib, M. Khan and H. Younus, *Protein J.*, 2007, **26**, 117–124.
9 A.-N. Spiess, N. Mueller and R. Ivell, *Clin. Chem.*, 2004, **50**, 1256–1259.
10 J. Hart, Z. Harris and S. Testa, *Biopolymers*, 2010, **93**, 1085–1092.
11 P. Del Vecchio, D. Esposito, L. Ricchi and G. Barone, *Int. J. Biol. Macromol.*, 1999, **24**, 361–369.
12 A. Mashaghi and A. Katan, *De Physicus*, 2013, **24e**, 59–61.
13 S. Ohtake and Y. Wang, *J. Pharm. Sci.*, 2011, **100**, 2020–2053.

14 Y.-P. Kim, M.-Y. Hong, J. Kim, E. Oh, H. K. Shon, D. W. Moon, H.-S. Kim and T. G. Lee, *Anal. Chem.*, 2007, **79**, 1377–1385.

15 Y. Mizuno, P. Carninci, Y. Okazaki, M. Tateno, J. Kawai, H. Amanuma, M. Muramatsu and Y. Hayashizaki, *Nucleic Acids Res.*, 1999, **27**, 1345–1349.

16 M. Wang, H. Yin, R. Landick, J. Gelles and S. Block, *Biophys. J.*, 1997, **72**, 1335–1346.

17 C. Bustamante, S. Smith, J. Liphardt and D. Smith, *Curr. Opin. Struct. Biol.*, 2000, **10**, 279–285.

18 I. Tessmer, C. G. Baumann, G. M. Skinner, J. E. Molloy, J. G. Hoggett, S. J. B. Tendler and S. Allen, *J. Mod. Opt.*, 2003, **50**, 1627–1636.

19 P. Gross, N. Laurens, L. B. Oddershede, U. Bockelmann, E. J. G. Peterman and G. J. L. Wuite, *Nat. Phys.*, 2011, **7**, 731–736.

20 A. Candelli, G. Wuite and E. Peterman, *Phys. Chem. Chem. Phys.*, 2011, **13**, 7263–7272.

21 M. Williams, J. Wenner, I. Rouzina and V. Bloomfield, *Biophys. J.*, 2001, **80**, 1932–1939.

22 P. Bechtluft, R. van Leeuwen, M. Tyreman, D. Tomkiewicz, N. Nouwen, H. Tepper, A. Driessen and S. Tans, *Science*, 2007, **318**, 1458–1461.

23 A. Mashaghi, P. Vach and S. Tans, *Rev. Sci. Instrum.*, 2011, **82**, 115103.

24 M. Manghi, N. Destainville and J. Palmeri, *Eur. Phys. J. E: Soft Matter Biol. Phys.*, 2012, **35**, 110.

25 D. A. Case, T. A. Darden, T. E. Cheatham III, C. L. Simmerling, J. Wang, R. E. Duke, R. Luo, R. C. Walker, W. Zhang and K. M. Merz, *et al.*, *AMBER 11*, University of California, San Francisco, 2010.

26 H. J. C. Berendsen, J. R. Grigera and T. P. Straatsma, *J. Phys. Chem.*, 1987, **91**, 6269–6271.

27 A. Pérez, I. Marchán, D. Svozil, J. Sponer, T. E. Cheatham III, C. A. Laughton and M. Orozco, *Biophys. J.*, 2007, **92**, 3817–3829.

28 K. N. Kirschner, A. B. Yongye, S. M. Tschampel, J. González-Outeiriño, C. R. Daniels, B. L. Foley and R. J. Woods, *J. Comput. Chem.*, 2008, **29**, 622–655.

29 H. J. C. Berendsen, J. P. M. Postma, W. F. v. Gunsteren, A. DiNola and J. R. Haak, *J. Chem. Phys.*, 1984, **81**, 3684–3690.

30 J.-P. Ryckaert, G. Ciccotti and H. J. C. Berendsen, *J. Comput. Phys.*, 1977, **23**, 327–341.

31 T. Darden, D. York and L. Pedersen, *J. Chem. Phys.*, 1993, **98**, 10089–10092.

32 L. L. C. Schrödinger, The PyMOL Molecular Graphics System, Version 1.3, 2010.

33 S. Smith, Y. Cui and C. Bustamante, *Science*, 1996, **271**, 795–799.

34 P. Cluzel, A. Lebrun, C. Heller, R. Lavery, J. Viovy, D. Chatenay and F. Caron, *Science*, 1996, **271**, 792–794.

35 J. F. Marko and E. D. Siggia, *Macromolecules*, 1995, **28**, 8759–8770.

36 G. A. King, P. Gross, U. Bockelmann, M. Modesti, G. J. L. Wuite and E. J. G. Peterman, *Proc. Natl. Acad. Sci. U. S. A.*, 2013, **110**, 3859–3864.

37 X. Zhang, H. Chen, S. Le, I. Rouzina, P. S. Doyle and J. Yan, *Proc. Natl. Acad. Sci. U. S. A.*, 2013, **110**, 3865–3870.

38 D. H. Paik and T. T. Perkins, *J. Am. Chem. Soc.*, 2011, **133**, 3219–3221.

39 S. Pal, L. Zhao and A. Zewail, *Proc. Natl. Acad. Sci. U. S. A.*, 2003, **100**, 8113–8118.

40 R. Dias, L. Magno, A. Valente, D. Das, P. Das, S. Maiti, M. Miguel and B. Lindman, *J. Phys. Chem. B*, 2008, **112**, 14446–14452.

41 P. Yakovchuk, E. Protozanova and M. D. Frank-Kamenetskii, *Nucleic Acids Res.*, 2006, **34**, 564–574.

42 I. Rouzina and V. Bloomfield, *Biophys. J.*, 1999, **77**, 3242–3251.

43 D. T. Haynie, *Biological Thermodynamics*, Cambridge University Press, 1st edn, 2001, pp. 160–163.

44 A. Godec and F. Merzel, *J. Am. Chem. Soc.*, 2012, **134**, 17574–17581.

45 D. Biswal, B. Jana, S. Pal and B. Bagchi, *J. Phys. Chem. B*, 2009, **113**, 4394–4399.

46 S. Garde and A. Patel, *Proc. Natl. Acad. Sci. U. S. A.*, 2011, **108**, 16491–16492.

47 Y. Koga, K. Nishikawa and P. Westh, *J. Phys. Chem. B*, 2007, **111**, 13943–13948.

48 D. Chandler, *Nature*, 2005, **437**, 640–647.

49 F. Stillinger, *Science*, 1980, **209**, 451–457.

50 K. R. Gallagher and K. A. Sharp, *J. Am. Chem. Soc.*, 2003, **125**, 9853–9860.

51 S. Sowerby, C. Cohn, W. Heckl and N. Holm, *Proc. Natl. Acad. Sci. U. S. A.*, 2001, **98**, 820–822.

52 K. Guckian, B. Schweitzer, R.-F. Ren, C. Sheils, D. Tahmassebi and E. Kool, *J. Am. Chem. Soc.*, 2000, **122**, 2213–2222.